ELSEVIER

Journal of Molecular Catalysis A: Chemical 161 (2000) 205–212

JOURNAL OF MOLECULAR CATALYSIS A: CHEMICAL

www.elsevier.com/locate/molcata

# Role of oxygen vacancy in the plasma-treated $TiO_2$ photocatalyst with visible light activity for NO removal

Isao Nakamura [a,*], Nobuaki Negishi [a], Shuzo Kutsuna [a], Tatsuhiko Ihara [b], Shinichi Sugihara [c], Koji Takeuchi [a,1]

[a] *National Institute for Resources and Environment, Tsukuba, Ibaraki 305-8569, Japan*
[b] *Department of Chemistry and Environment Technology, Kinki University, Higashi-hiroshima, Hiroshima 739-2116, Japan*
[c] *Ecodevice Co. Ltd., 3-26-2 Ryogoku, Sumida-ku, Tokyo 130-0026, Japan*

Received 23 February 2000; accepted 23 June 2000

**Abstract**

The photocatalytic activity for NO removal under an oxidative atmosphere has been studied over commercial $TiO_2$ and plasma-treated $TiO_2$ powders. By the plasma treatment, the photocatalytic activity for NO removal appeared in the visible light region up to 600 nm without a decrease in the ultraviolet light activity. It was found that the NO was removed as nitrate ($NO_3^-$) by photocatalytic oxidation over the $TiO_2$ powders, where $NO_3^-$ was accumulated. No difference in the crystal structure, the crystallinity, and the specific surface area was observed between the raw $TiO_2$ and the plasma-treated $TiO_2$ photocatalysts. In electron spin resonance (ESR) measurements, a sharp signal at $g = 2.004$, which was identified as the electrons trapped on oxygen vacancies, was detected only for plasma-treated $TiO_2$ under visible light irradiation. The saturated intensity of the ESR signal at $g = 2.004$ was proportional to the removal percentage of nitrogen oxides, suggesting that the number of trapped electrons determined the activity for the photocatalytic oxidation of NO to $NO_3^-$. The appearance of the visible light activity in the plasma-treated $TiO_2$ photocatalyst was ascribed to the newly formed oxygen vacancy state between the valence and the conduction bands in the $TiO_2$ band structure. 

*Keywords:* Photocatalysis; Titanium dioxide; Nitric oxide; Visible light activity; Oxygen vacancy

## 1. Introduction

It is well known that $TiO_2$ shows excellent photocatalytic activity for oxidative degradation of environmental pollutants [1,2]. Recently, this has been applied to removal of atmospheric nitrogen oxides ($NO_x$) which cause acid rain [3–7]. We have previously reported that the $TiO_2$ photocatalyst containing activated carbon oxidizes 1–2 ppm $NO_x$ in air to $HNO_3$ very rapidly [3]. However, it is necessary to irradiate with ultraviolet light of wavelengths shorter than about 380 nm in order to activate $TiO_2$ as a photocatalyst, because $TiO_2$ is a semiconductor oxide with a relatively large band gap of 3.2 eV [8,9]. Thus, when using sunlight to activate the $TiO_2$ photocatalyst for $NO_x$ removal on a large scale, only a small percentage of the energy in sunlight is avail-

* Corresponding author. Tel.: +81-298-618169; fax: +81-298-618158.
*E-mail addresses:* nakamura@nire.go.jp (I. Nakamura), takeuchi@nire.go.jp (K. Takeuchi).
[1] Co-corresponding author.

1381-1169/00/$ - see front matter 
PII: S1381-1169(00)00362-9

able. For practical use, it is essential to develop photocatalysts with visible light activity.

Extensive research has been conducted on the development of a $TiO_2$ photocatalyst operating under visible light irradiation [6,7,10–20]. The visible light response due to the spectral sensitization of organic dyes has been studied [10–13], and attempts to elongate the lifetime of employed dyes are currently carried out by numerous researchers. $TiO_2$ photocatalysts doped with transition metals such as Cr, Mn, Co, Fe, etc. have been found to absorb visible light [14–20]. Matsumoto et al. [14] have shown that Co-doped polycrystalline $TiO_2$ electrodes prepared at 673–823 K show an apparent visible light response (420–550 nm). They explained that the response is based on the newly formed d-band by the interaction of the interstitial Co ion in the $TiO_2$ lattice. Ghosh and Maruska [16] have also found that the presence of Cr gives rise to optical absorption extending from the fundamental band edge of $TiO_2$ at 415 nm to well past 550 nm, a wavelength region containing a major portion of the solar radiation.

However, in most cases, the primary ultraviolet activity of the $TiO_2$ photocatalyst tends to decrease, because the doped metals act as an electron–hole recombination center [20,21]. Pichat et al. [20] reported that the doping of $Cr^{3+}$ ion in $TiO_2$ brought about drastic decreases in the activity for photocatalytic oxidations (oxalic acid, propane, or 2-propanol oxidation) and in photoinduced oxygen isotope exchange, although the Cr-doped $TiO_2$ absorbed visible light. Therefore, no net increase in the photoactivity of doped $TiO_2$ is observed.

Anpo et al. [6,7] prepared a $TiO_2$ photocatalyst which was able to absorb visible light due to the implantation of Cr ion. It is shown that the decomposition of NO into $N_2$, $O_2$, and $N_2O$ proceeds on the Cr ion-implanted $TiO_2$ photocatalyst under oxygen-free conditions and visible light irradiation above 450 nm. Furthermore, they have confirmed that the Cr ion-implanted $TiO_2$ catalyst shows exactly the same photocatalytic efficiency as the original $TiO_2$ catalyst under ultraviolet light irradiation.

On the other hand, as we noted in the reports that the slightly reduced $TiO_2$ gains an absorption in the visible light region [22], and the surface of powder materials can be modified by a low-temperature plasma treatment [23], we attempted to treat a $TiO_2$ powder with the plasma using a reducing gas. We have recently succeeded in preparing a $TiO_2$ powder that can absorb visible light as a result of hydrogen plasma treatment using radio-frequency discharge [24]. The characteristic of this method is that a slightly reduced $TiO_2$ can be prepared relatively simply without other materials except for $TiO_2$.

As previously mentioned, we have found that $NO_x$ can be removed over the $TiO_2$-based photocatalyst under black light irradiation (wavelength: 300–400 nm) [3]. If the photocatalytic reaction of NO removal proceeds over the plasma-treated $TiO_2$ powder under visible light irradiation above 400 nm without a decrease in the ultraviolet light activity, this will greatly enhance the efficiency of the catalyst under the sun. In this study, we have examined the photocatalytic activity of plasma-treated $TiO_2$ for NO removal under visible light irradiation and have investigated the cause for the appearance of the visible light photocatalytic activity.

## 2. Experimental

The $TiO_2$ sample used in this study was ST-01 obtained from Ishihara Sangyo Kaisha (100% anatase, crystallite size of 7 nm, nominal specific surface area of 300 $m^2\,g^{-1}$). The plasma-treated $TiO_2$ samples were prepared by radio-frequency discharge (13.56 MHz, 500 W) under 2 Torr $H_2$ at 673 K for 10–60 min in a quartz glass chamber. The color of the sample powder was changed from white to light yellow by the treatment.

The flow reactor consisted of a Pyrex glass vessel ($\sim$ 500 $cm^3$) equipped with a Jasco SM-5 monochromatic light source using a 300 W xenon lamp was used to study the photocatalytic reaction of NO removal. The monochromatic light source allows us to irradiate only the light of the desired wavelength with a full width at half-maximum (FWHM) of 20 nm on to the powder catalyst. The UV-A irradiance (315–400 nm) was about 0.03 mW $cm^{-2}$ at the $TiO_2$ photocatalyst located in the vessel. The NO removal reaction was carried out at room temperature using a gas mixture of dry air containing 1.0 ppm NO, which was produced by a STEC SGPU-22 air purifier and 50 ppm of $NO/N_2$ from a cylinder purchased from Takachiho Chemicals Co. The reac-

tion gas mixture passed through the vessel containing $TiO_2$ powder (0.20 g) at a flow rate of 1500 ml $min^{-1}$ and a total pressure of 760 Torr. The NO and $NO_2$ concentrations were continuously monitored with an on-line chemiluminescent $NO_x$ analyzer (Monitor Labs 8840). It was confirmed that no removal of NO was observed in a blank test, i.e. in a reaction without the $TiO_2$ photocatalyst.

X-ray diffraction (XRD) analysis was performed with a Rotarflex RU-300 using CuK$\alpha$ radiation. The specific surface area of the catalyst, which had been degassed at 393 K under He for 1 h, was measured using a Quantachrome AS-1 by the Brunauer–Emmett–Teller method with $N_2$ adsorption at 77 K. The UV–VIS absorption spectra of the samples were obtained with a Shimadzu UV-2500PC spectrometer equipped with an integrating sphere.

For the electron spin resonance (ESR) measurements, a 0.10 g portion of $TiO_2$ powder was placed in a Suprasil quartz-glass sample tube, which was then evacuated to $< 1 \times 10^{-3}$ Torr. After the evacuation, 760 Torr of high-purity $N_2$ (99.999%, Takachiho Chemicals Co.) gas was introduced into the sample tube which was sealed. The ESR spectra were obtained at 77 K with a JEOL JES-TE300 ESR spectrometer coupled with a computer for data acquisition and instrument control. The $g$ value and the signal intensity were corrected by a $Mn^{2+}$ marker. The settings for the ESR spectrometer were: center field 330,00 mT; modulation frequency 100 kHz; microwave frequency 9.22 GHz; power 1.00 mW. The photoirradiation on the sample in the ESR cavity was carried out using a SAN-El SUPER BRIGHT-152S fiber-optic light source with a 150 W xenon lamp through a longpass glass filter (Schott GG420, GG475, OG515, OG570). The variation in light intensity with wavelength was not corrected in this study.

## 3. Results and discussion

### 3.1. Photocatalytic activity of raw $TiO_2$ and plasma-treated $TiO_2$

The photocatalytic reaction of NO removal was carried out over raw $TiO_2$ and plasma-treated $TiO_2$ powders in order to examine the effect of the plasma treatment on the visible light activity. Fig. 1 shows the dependence of the $NO_x$ removal percentage on the irradiation wavelength over raw $TiO_2$ and plasma-treated $TiO_2$ powder photocatalysts (treatment times: 10, 20, 60 min). The $NO_x$ removal percentage was calculated as the ratio of the net $NO_x$ removed for 1 h at each wavelength as follows:

$$NO_x \text{ removal}\,(\%) = \frac{\int ([NO]_{\text{decreased}} - [NO_2]_{\text{formed}})\,dt}{\int [NO]_{\text{supplied}}\,dt} \times 100$$

As for raw $TiO_2$, the removal percentage was zero at wavelengths longer than 450 nm. Below 450 nm, the percentage increased linearly with decreasing wavelength. A $NO_x$ removal percentage of 13% was obtained at 360 nm. The formation of $NO_2$ was observed only under the illumination of ultraviolet light. On the other hand, for plasma-treated $TiO_2$, NO removal was observed up to ca. 600 nm. The removal percentage increased linearly with decreasing wavelength between 450 and 600 nm, and below 450 nm, it was almost constant or increased slightly. About 20% of the removal percentage was seen at

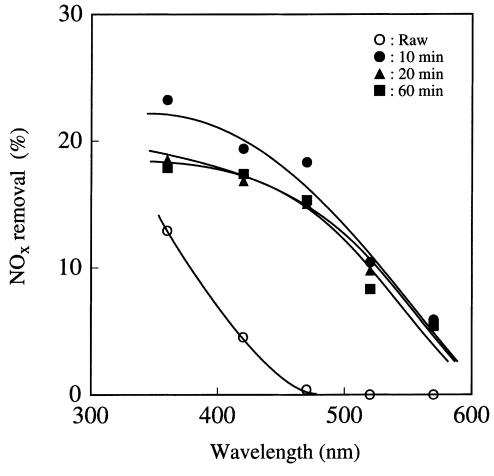


Fig. 1. $NO_x$ removal percentage as a function of irradiation wavelength over the raw $TiO_2$ and the plasma-treated $TiO_2$ photocatalysts.

360 nm in every plasma-treated sample. It is clearly shown that the plasma-treated $TiO_2$ powder has a visible light photocatalytic activity for NO removal, and furthermore, the removal percentage in the ultraviolet light region increases slightly, compared with the raw $TiO_2$ powder. However, the plasma treatment time did not produce a remarkable difference in the removal percentage. It is found that the $TiO_2$ photocatalyst with visible light activity is sufficiently prepared even with a plasma treatment time of 10 min.

The reaction products in the NO removal were examined by ion chromatography (Shimadzu HIC-6A). The post-reaction $TiO_2$ powder was immersed in a 30 ml portion of purified water, and the mixture was then stirred using an ultrasonic bath for 1 min. Nitrate ($NO_3^-$) and trace amounts of nitrite ($< 2\%$ of the amount of detected $NO_3^-$) were detected in the mixture. The total amount of $NO_3^-$ in the mixture was close to that estimated from the $NO_x$ removal percentage. Furthermore, in the infrared spectroscopy measurement, the peaks characteristic of the chelating and the bridging bidentate $NO_3^-$ on $TiO_2$ have been observed during the reaction, which will be published elsewhere. The intensity of the peaks increased with the reaction time. It was thus indicated that the NO was converted to $NO_3^-$ by photocatalytic oxidation over the $TiO_2$ powders and that $NO_3^-$ was accumulated on the catalyst surface.

### *3.2. XRD analysis and UV–VIS absorption measurements of raw $TiO_2$ and plasma-treated $TiO_2$*

The crystal structure of the $TiO_2$ powder was examined using XRD. Fig. 2 shows the XRD patterns for the raw $TiO_2$ and the plasma-treated $TiO_2$ powder photocatalysts (treatment times: 10, 20, 60 min). Only the peaks identified as an anatase structure were observed in the raw $TiO_2$ powder [9]. In the case of the plasma-treated $TiO_2$ powder, only the anatase structure was also found without any contamination from other phases such as a rutile structure, regardless of the treatment time. Furthermore, both the intensity and the FWHM of the peaks in plasma-treated $TiO_2$ were almost same as those in raw $TiO_2$. These results indicate that both the crystal structure and the crystallinity of $TiO_2$ do not change

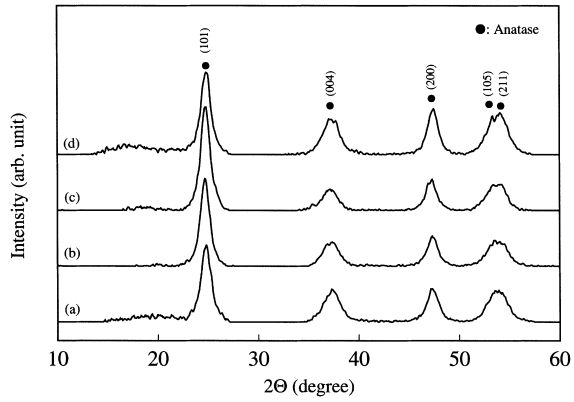


Fig. 2. XRD patterns of (a) raw $TiO_2$, and plasma-treated $TiO_2$ for (b) 10 min, (c) 20 min, and (d) 60 min.

due to the radio-frequency plasma treatment. The specific surface areas of raw $TiO_2$ and plasma-treated $TiO_2$ for 10, 20, and 60 min were determined to be 279.5, 270.3, 264.9, and 270.7 $m^2\,g^{-1}$, respectively. No significant difference was observed in the specific surface area between raw $TiO_2$ and plasma-treated $TiO_2$. In contrast, the appearance of a rutile structure and a remarkable decrease in specific surface area were observed for the $TiO_2$ powder prepared by the hydrogen plasma using a microwave discharge, in which controlling the treatment temperature of the sample was very difficult. The microwave plasma-treated $TiO_2$ showed little visible light activity for NO removal.

The UV–VIS absorption spectra of raw and plasma-treated $TiO_2$ (treatment times: 10, 20, 60 min) are shown in Fig. 3. For raw $TiO_2$, no absorption was observed above the wavelength of 420 nm. The plasma-treated $TiO_2$ powders exhibited a new absorption in the visible light region at wavelengths longer than 420 nm. The edges of the absorption shifted to approximately 600 nm, which was in good agreement with the activity for photocatalytic oxidation of NO in this region (Fig. 1). Light absorption is a necessary condition for a photocatalyst to function, although it is not a sufficient condition. It was thus concluded that the new absorption band at 400–600 nm induced the visible light activity of the plasma-treated $TiO_2$ photocatalyst. Breckenridge and Hosler have reported that the slightly reduced $TiO_2$ has an absorption in the visible light region [22]. It is suggested that the hydrogen plasma-treated $TiO_2$

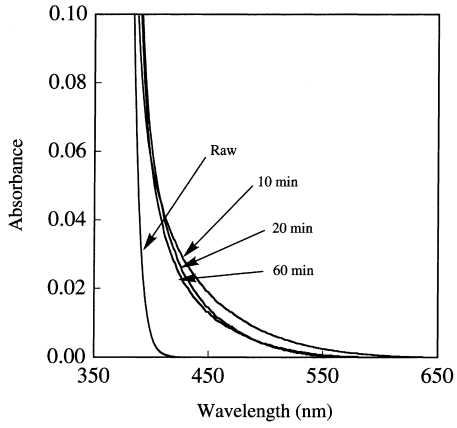


Fig. 3. UV–VIS absorption spectra of raw and plasma-treated $TiO_2$ for 10, 20, and 60 min.

powder is somewhat reduced. The appearance of the visible light absorption by the plasma treatment may be due to the change in the electronic state of the $TiO_2$ photocatalyst caused by the reduction.

### 3.3. ESR measurements for plasma-treated $TiO_2$

To further characterize the plasma-treated $TiO_2$ photocatalyst, ESR measurements were performed under visible light irradiation. Fig. 4(a) and (b) show the ESR spectra of the plasma-treated (60 min) $TiO_2$ powder obtained under the dark condition and with $>475$ nm light irradiation for 5 min, respectively. Both spectra were recorded at 77 K. In addition, spectrum (c), obtained by subtracting spectrum (a) from spectrum (b), is also shown in Fig. 4. The signals similar to those observed in the plasma-treated sample under the dark condition are also detected for the raw $TiO_2$ powder as shown in Fig. 5(a), although the identification of these signals has not been achieved. Probably, these signals are characteristic of the ST-01 sample, because such signals are not observed for Degussa P-25 samples.

As a result of the visible light irradiation for plasma-treated $TiO_2$, a symmetrical, sharp signal appeared at $g = 2.004$ as shown in Fig. 4(c), where no other signal such as $Ti^{3+}$ ($g = 1.96$) [25–30] and $O_2^-$ ($g_1 = 2.025$, $g_2 = 2.009$, and $g_3 = 2.003$) [31] were detected for a 1 h irradiation. On the other hand, for the raw $TiO_2$ powder, no change in the ESR spectra was observed under the visible light irradiation (Fig. 5(c)); that is, the signal at $g = 2.004$ was detected only for the plasma-treated sample.

The ESR spectra of vacuum-reduced $TiO_2$ at 673–773 K were reported by Serwicka et al. [25,26]. They observed a broad signal assigned to $Ti^{3+}$ ions ($g \sim 1.96$) and a sharp signal at $g = 2.003$. They attributed the latter signal to a bulk defect, probably an electron trapped on an oxygen vacancy. Volodin et al. [32–34] also observed the singlet signal at $g = 2.0035$ for reduced $TiO_2$. They concluded that the signal was due to the surface defects (S-centers). Naccache et al. [35] reported that the symmetrical line at $g = 2.003$ detected on reduced $TiO_2$ arose from the localization of a conduction electron in the lattice. Also, on $MoO_3$ after evacuation, a sharp signal at $g = 2.001$ has been observed, which is assigned to an F-center [36]. Based on these literature data for the ESR signal, the signal at $g = 2.004$ newly observed here by the visible light irradiation for the plasma-treated $TiO_2$ powder was assigned to the electron trapped on the oxygen vacancy. It was

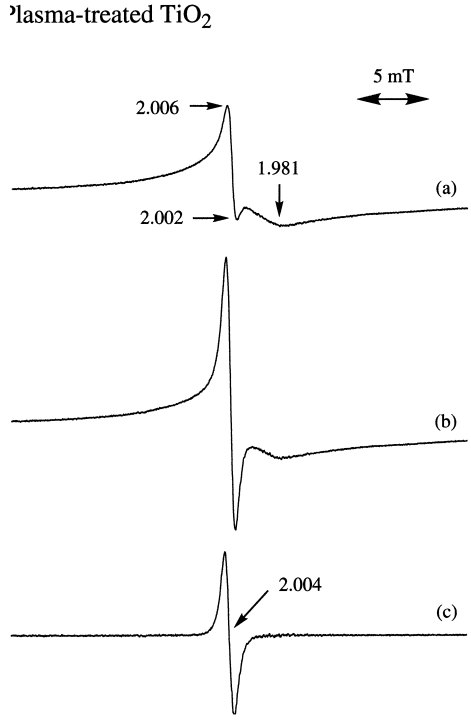


Fig. 4. ESR spectra of plasma-treated $TiO_2$ under (a) the dark condition, (b) $>475$ nm light irradiation for 5 min, and (c) corresponds to spectrum in (b) − spectrum in (a).

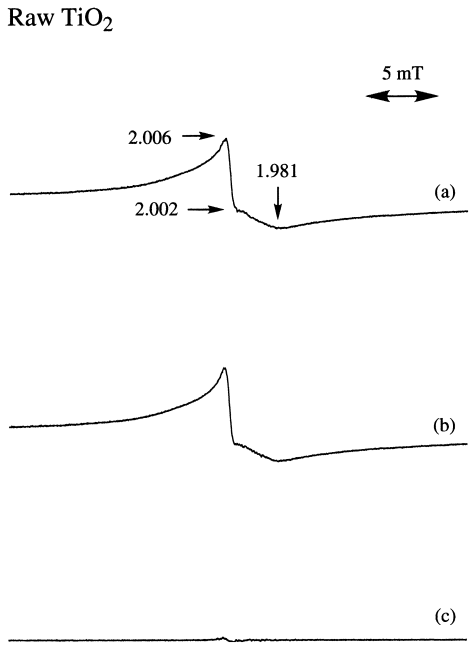


Fig. 5. ESR spectra of raw $TiO_2$ under (a) the dark condition, (b) $>475$ nm light irradiation for 5 min, and (c) corresponds to spectrum in (b) − spectrum in (a).

considered that the oxygen vacancies were formed in the crystal lattice of $TiO_2$ by the plasma treatment, maintaining the anatase structure.

Fig. 6 shows the ESR signal intensity of the electrons trapped on oxygen vacancies ($g = 2.004$) as a function of the irradiation time at various visible light wavelengths ($>420$, $>475$, $>515$, $>570$ nm). The identical sample was used in this experiment. For the wavelengths of $>475$ and $>570$ nm, the experiments were performed twice to check the reproducibility. In all wavelengths, the signal intensity increased with the irradiation time up to approximately 40 min and then became saturated. Each saturated plateau remained at least 2 h after stopping the illumination, indicating that the decay of the trapped electrons observed here were negligible. Thus, the saturation intensity is clearly not influenced by the number of photons depending on the wavelength, though the number of photons may determine the time until saturation.

The saturated plateau became higher with shorter wavelengths of the irradiation, indicating that more electrons were produced and trapped on the oxygen vacancies at a shorter wavelength. If the oxygen vacancy state has a unique energy level, the number of trapped electrons does not vary with the excitation wavelength. It has been reported that the two different oxygen vacancy states between the valence and the conduction bands exist in the reduced $TiO_2$ single crystal [37]. Sanz et al. [38] have also observed some defect states, which were assigned to oxygen vacancies caused by the preferential removal of oxygen during the sputtering of $ZrO_2$ with $Ar^+$ bombardment. If the oxygen vacancy states with some different energy levels exist in plasma-treated $TiO_2$ as reported in these papers, the phenomenon in Fig. 6 in which the number of trapped electrons varies with excitation wavelength may be explicable. However, a further investigation will be needed for a reasonable explanation of the phenomenon.

The electrons trapped on oxygen vacancies are considered to be closely related to the photocatalytic oxidation of NO under visible light irradiation. Fig. 7 shows the $NO_x$ removal percentage as a function of the saturated intensity of the ESR signal at $g = 2.004$ observed at various visible light irradiations. It is clearly shown that the $NO_x$ removal percentage is proportional to the ESR signal intensity. That is, the number of the trapped electrons is well correlated with the photocatalytic activity for the NO oxidation. It is also noted that the straight line fitted to the data points passes through the origin. This result indicates

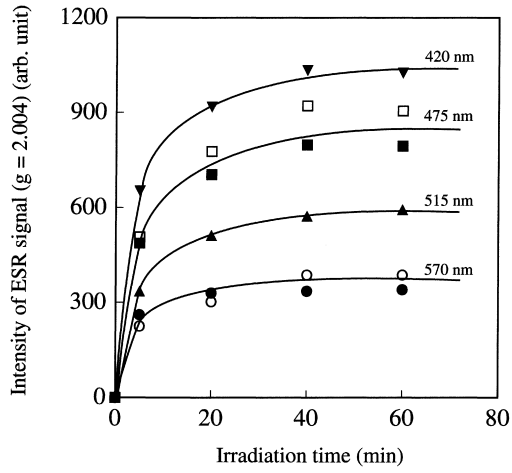


Fig. 6. Intensity of the ESR signal at $g = 2.004$ due to the electrons trapped on the oxygen vacancy as a function of the irradiation time at various visible light wavelengths.

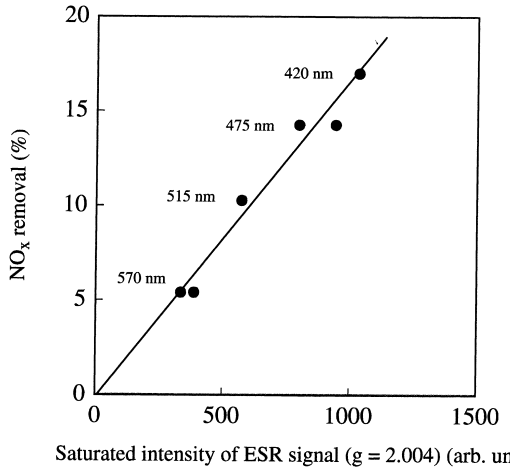


Fig. 7. $NO_x$ removal percentage as a function of the saturated intensity of the ESR signal at $g = 2.004$ observed at various visible light irradiations.

that the photocatalytic oxidation of NO to $NO_3^-$ does not proceed without the trapped electrons. As shown in Fig. 8, from the relationship between the wavelength and the ESR signal intensity, the wavelength, above which the trapped electrons were not observed, was estimated to be 639 nm. This wavelength is quite comparable to those observed in the $NO_x$ removal percentage (Fig. 1) and in the UV–VIS absorption (Fig. 3).

There have been a number of investigations concerning the energy level of oxygen vacancies [37,39].

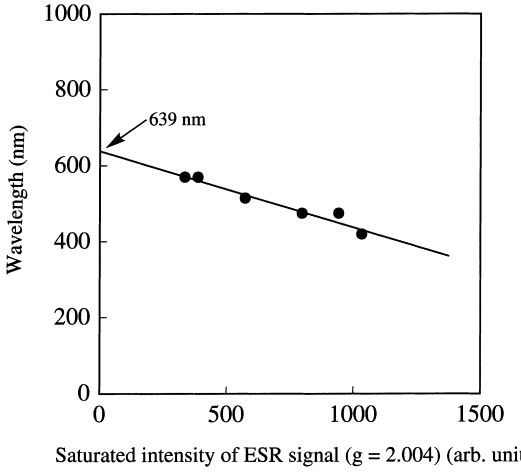


Fig. 8. The relationship between the irradiation wavelength and the saturated intensity of the ESR signal at $g = 2.004$.

Cronemeyer [37] measured the ionization energy for electrons ionized from an oxygen vacancy in the $TiO_2$ single crystal, which was reduced in hydrogen at about 973 K for several minutes. The ionization energy, i.e. the bandgap energy between the conduction band and the oxygen vacancy states, was determined to be 0.75–1.18 eV for the reduced $TiO_2$ sample. Based on this value, the band structure model for the anatase $TiO_2$ with oxygen vacancies was constructed, as shown in Fig. 9. The oxygen vacancy states in anatase $TiO_2$ were determined to be located 2.02–2.45 eV above the valence band. This bandgap energy corresponds to a wavelength of 506–614 nm, which is close to that needed to produce the electron on the oxygen vacancy in the plasma-treated $TiO_2$ powder (Fig. 8). By treating the $TiO_2$ powder in the hydrogen plasma, oxygen vacancies are created, and the oxygen vacancy states between the valence and the conduction bands are newly formed in the $TiO_2$ band structure. It is expected that the oxygen vacancy states take part in a new photoexcitation process. That is, the electron may be excited to the oxygen vacancy states from the valence band even with the energy of visible light. The activation of oxygen, especially the formation of $O^-$, is considered to be very important for photocatalytic oxidation processes [40]. Therefore, it is presumed that the electrons excited to the oxygen vacancy state or the holes formed in the valence band perhaps react with $O_2$ or oxygen species and produce the reactive oxygen species such as $O^-$ or atomic oxygen, which will participate in the oxidation process of NO to $NO_3^-$.

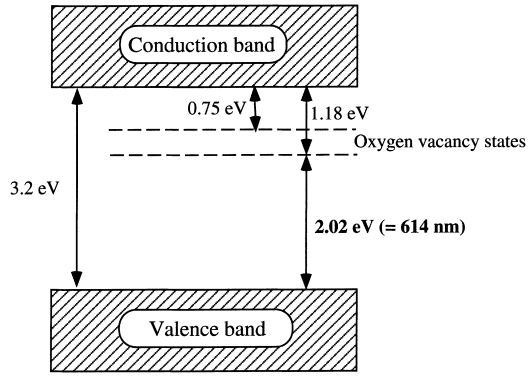


Fig. 9. A proposed band structure model for the anatase $TiO_2$ with oxygen vacancies.

## 4. Conclusions

The hydrogen plasma-treated $TiO_2$ photocatalyst showed visible light activity for NO removal under an oxidative atmosphere, where the NO was removed as $NO_3^-$ accumulated on the catalyst surface. Neither the crystal structure nor the specific surface area was observed to change between the raw $TiO_2$ and the plasma-treated $TiO_2$ photocatalysts. The electrons trapped on oxygen vacancies in plasma-treated $TiO_2$ were detected under visible light irradiation. The number of electrons trapped on oxygen vacancies was proportional to the $NO_x$ removal percentage, suggesting that the number of trapped electrons determined the activity for the photocatalytic oxidation of NO to $NO_3^-$. The appearance of the visible light photocatalytic activity in plasma-treated $TiO_2$ is due to a new photoexcitation process by the formation of the oxygen vacancy state located between the valence and the conduction bands.

## Acknowledgements

This work was supported by the New Energy and Industrial Technology Development Organization (NEDO) under the contract No. 98K09-014.

## References

[1] M.A. Fox, M.T. Dulay, Chem. Rev. 93 (1993) 341.
[2] M.R. Hoffmann, S.T. Martin, W. Choi, D.W. Bahnemann, Chem. Rev. 95 (1995) 69.
[3] T. Ibusuki, K. Takeuchi, J. Mol. Catal. 88 (1994) 93.
[4] N. Negishi, K. Takeuchi, T. Ibusuki, J. Mater. Sci. 33 (1998) 5789.
[5] K. Takeuchi, J. Jpn. Soc. Atmos. Environ. 33 (1998) 139.
[6] M. Anpo, Catal. Surv. Jpn. 1 (1997) 169.
[7] M. Anpo, Y. Ichihashi, M. Takeuchi, H. Yamashita, Res. Chem. Intermed. 24 (1998) 143.
[8] H. Tang, H. Berger, P.E. Schmid, F. Lévy, G. Burri, Solid State Commun. 87 (1993) 847.
[9] H. Tang, K. Prasad, R. Sanjines, P.E. Schmid, F. Lévy, J. Appl. Phys. 75 (1994) 2042.
[10] K. Hashimoto, T. Kawai, T. Sakata, Chem. Lett. (1983) 709.
[11] B. O'Regan, M. Grätzel, Nature 353 (1991) 737.
[12] M.K. Nazeeruddin, A. Kay, I. Rodicio, R. Humphry-Baker, E. Müller, P. Liska, N. Vlachopoulos, M. Grätzel, J. Am. Chem. Soc. 115 (1993) 6382.
[13] H. Yanagi, Y. Ohoka, T. Hishiki, K. Ajito, A. Fujishima, Appl. Surf. Sci. 113/114 (1997) 426.
[14] Y. Matsumoto, J. Kurimoto, Y. Amagasaki, E. Sato, J. Electrochem. Soc. 127 (1980) 2148.
[15] Y. Matsumoto, J. Kurimoto, T. Shimizu, E. Sato, J. Electrochem. Soc. 128 (1981) 1040.
[16] A.K. Ghosh, H.P. Maruska, J. Electrochem. Soc. 124 (1977) 1516.
[17] E. Borgarello, J. Kiwi, M. Grätzel, E. Pelizzetti, M. Visca, J. Am. Chem. Soc. 104 (1982) 2996.
[18] W.K. Wong, M.A. Malati, Solar Energy 36 (1986) 163.
[19] T.R.N. Kutty, M. Avudaithai, Chem. Phys. Lett. 163 (1989) 93.
[20] J.M. Herrmann, J. Disdier, P. Pichat, Chem. Phys. Lett. 108 (1984) 618.
[21] Z. Luo, Q.H. Gao, J. Photochem. Photobiol. A: Chem. 63 (1992) 367.
[22] R.G. Breckenridge, W.R. Hosler, Phys. Rev. 91 (1953) 793.
[23] T. Ihara, S. Kawamura, M. Kiboku, Y. Iriyama, Prog. Organic Coatings 31 (1977) 133.
[24] K. Takeuchi, I. Nakamura, O. Matsumoto, S. Sugihara, M. Andoh, T. Ihara, Chem. Lett., subrnitted for publication.
[25] E. Serwicka, M.W. Schlierkamp, R.N. Schindler, Z. Naturforsch. Teil A 36 (1981) 226.
[26] E. Serwicka, Colloids Surf. 13 (1985) 287.
[27] A.R. González-Elipe, J. Soria, G. Munuera, Chem. Phys. Lett. 57 (1978) 265.
[28] M. Anpo, T. Shima, S. Kodama, Y. Kubokawa, J. Phys. Chem. 91 (1987) 4305.
[29] V.A. Poluboyarov, G.A. Dergaleva, V.F. Anufrienko, S.N. Pavlova, V.A. Sazonov, V.V. Popovskii, G.A. Zenkovets, Kinet. Catal. 30 (1989) 612.
[30] Y. Nakaoka, Y. Nosaka, J. Photochem. Photobiol. A: Chem. 110 (1997) 299.
[31] R.F. Howe, M. Grätzel, J. Phys. Chem. 91 (1987) 3906.
[32] A.M. Volodin, A.E. Cherkashin, V.S. Zakharenko, React. Kinet. Catal. Lett. 11 (1979) 103.
[33] A.M. Volodin, A.E. Cherkashin, V.S. Zaldiarenko, React. Kinet. Catal. Lett. 11 (1979) 107.
[34] A.M. Volodin, A.E. Cherkashin, V.S. Zakharenko, React. Kinet. Catal. Lett. 11 (1979) 221.
[35] C. Naccache, P. Meriaudeau, M. Che, A.J. Tench, Trans. Faraday Soc. 67 (1971) 506.
[36] P.F. Cornaz, J.H.C. van Hooff, F.J. Pluijm, G.C.A. Schuit, Disc. Faraday Soc. 41 (1966) 290.
[37] D.C. Cronemeyer, Phys. Rev. 113 (1959) 1222.
[38] J.M. Sanz, A.R. González-Elipe, A. Fernández, D. Leinen, L. Galán, A. Stampfl, A.M. Bradshaw, Surf. Sci. 307/309 (1994) 848.
[39] S. Sazonova, T.P. Khokhlova, G.M. Sushentseva, N.P. Keier, Kinet. Katiliz 3 (1962) 655.
[40] M. Formenti, S.J. Teichner, Catalysis (London) 2 (1979) 87.